Supporting Information

The Adsorption of Europium and Uranium on the Sodium Dodecyl Sulfate Modified Molybdenum Disulfide Composites

Jian Wang*, Shanye Yang, Gong Cheng, Pengcheng Gu

MOE Key Laboratory of Resources and Environmental System Optimization, College of Environmental Science and Engineering, North China Electric Power University, Beijing, 102206, P.R. China

*: Corresponding author. Email: wangjian@ncepu.edu.cn (J. Wang).

The pseudo-first-order kinetic model can be described as:[1]

$$ln(q_e - q_t) = ln\, q_e - k_1 t \quad (1)$$

The pseudo-second-order kinetic model can be expressed as:[1]

$$q_t = \frac{k_2 q_e^2 t}{1 + k_2 q_e t} \quad (2)$$

where k_1 and k_2 are the pseudo-first-order and pseudo-second-order rate constants, q_e and q_t (mg/g) are the adsorption of radionuclides at equilibrium and time t (min).

The Langmuir model can be defined as:[2]

$$q_e = \frac{Q_0 C_e b}{1 + C_e b} \quad (3)$$

The Freundlich model is expressed as:[2]

$$q_e = K_f C_e^{1/n} \quad (4)$$

The Sips model can expressed as:[1]

$$q_e = \frac{Q_0 (K_s C_e)^m}{1 + (K_s C_e)^m} \quad (5)$$

The Redlich-Peterson model is defined as:[1]

$$q_e = \frac{K_R C_e}{1 + a_R C_e^{\beta}} \quad (6)$$

where C_e is the equilibrium concentration of adsorbate in solution, Q_0 represents the theoretical saturated adsorption capacity, K_R and a_R are Redlich-Peterson constants, K_S is the affinity constant, n denotes Freundlich coefficient, m is the Sips parameter for surface heterogeneity description, K_f and b are constant, q_e is the removal capacity at equilibrium.

The free energy change ΔG^0 (kJ/mol), standard entropy change ΔS^0 (J/(mol·K)), and standard enthalpy change ΔH^0 (kJ/mol) can be calculated from the following equations [1]:

$$Kc = \frac{C_{Ae}}{C_e} \tag{7}$$

$$\Delta G^0 = -RT \ln Kc \tag{8}$$

$$\ln Kc = \frac{\Delta S^0}{R} - \frac{\Delta H^0}{RT} \tag{9}$$

where Kc is the thermodynamic equilibrium constant; C_e (mg/L) and C_{Ae} (mg/L) denote the equilibrium concentration of radionuclides in aqueous solutions and amount of radionuclides adsorbed on the composites, respectively; T (K) is Kelvin temperature; R (8.314 J/(mol·K)) is the ideal gas constant.

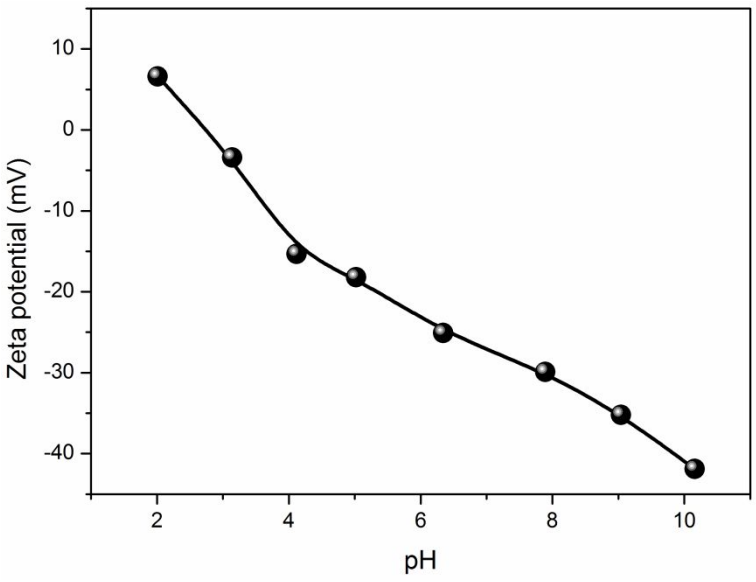

Figure S1. Zeta potential of SDS/MoS_2.

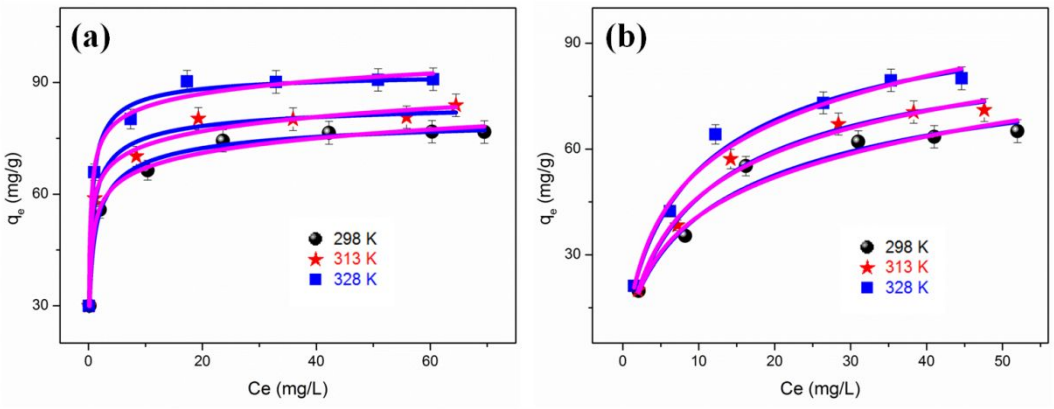

Figure S2. Adsorption isotherms for Eu(III) (a) and U(VI) (b) (the blue lines represent the Sips model, the magenta lines represent the Redlich-Peterson model, pH = 5.0 ± 0.1, I = 0.01 M NaCl, m/V = 0.25 g/L, adsorption time = 10 h).

Table S1. The adsorption time of SDS/MoS_2 compared with other materials.

Pollutant	Adsorbent	Time (min)	Reference
Eu(III)	FeNi-RGO complexes	2400	3
Eu(III)	Al-MCM-41	720	4
Eu(III)	Magnetic GOs	540	5
Eu(III)	CMC/MMWCNTs composites	600	6
Eu(III)	SDS/MoS_2	300	This study
U(VI)	Pyrite	8640	7
U(VI)	GPNB-BT	720	8
U(VI)	Pal/PAO	300	9
U(VI)	4XADMnO	390	10
U(VI)	SDS/MoS_2	180	This study

References

(1) Tangsir, S.; Hafshejani, L.D.; Lahde, A.; Marja, M.; Hooshmand, A.; Naseri, A.A.; Moazed, H.; Jokiniemi, J.; Bhatnagar, A. Water defluoridation using Al_2O_3 nanoparticles synthesized by flame spray pyrolysis (FSP) method, *Chem. Eng. J.* **2016**, *288*, 198-206.

(2) Yu, X.; Tong, S.; Ge, M.; Zuo, J.; Cao, C.; Song, W. One-step synthesis of magnetic composites of cellulose@iron oxide nanoparticles for arsenic removal, *J. Mater. Chem. A* **2013**, *1*, 959-965.

(3) Qi, W.; Tian, L.; Liu, B.; Lin, J.; Liu, D.; Tu, P.; Liu, P.; Li, Z.; Chen, X.; Wu, W. Adsorption of Eu(III) on defective magnetic FeNi/RGO composites: effect of pH, ion strength, ions and humic acid, *J. Radioanal. Nucl. Ch.* **2015**, *303*, 2211-2220.

(4) Zuo, L.; Yu, S.; Zhou, H.; Jiang, J.; Tian, X. Adsorption of Eu(III) from aqueous solution using mesoporous molecular sieve, *J. Radioanal. Nucl. Ch.* **2011**, *288*, 579-586.

(5) Li, D.; Zhang, B.; Xuan, F. The sorption of Eu(III) from aqueous solutions by magnetic graphene oxides: a combined experimental and modeling studies, *J. Mol. Liq.* **2015**, *211*, 203-209.

(6) Zong, P.; Cao, D.; Cheng, Y.; Wang, S.; Hayat, T.; Alharbi, N.S.; Guo, Z.; Zhao, Y.; He, C. Enhanced performance for Eu(III) ion remediation using magnetic multiwalled carbon nanotubes functionalized with carboxymethyl cellulose nanoparticles synthesized by plasma technology, *Inorg. Chem. Front.* **2018**, *5*, 3184-3196.

(7) Liu, H.; Zhu, Y.; Xu, B.; Li, P.; Sun, Y.; Chen, T. Mechanical investigation of U(VI) on pyrrhotite by batch, EXAFS and modeling techniques, *J. Hazard. Mater.* **2017**, *322*, 488-498.

(8) Meng, J.; Lin, X.; Li, H.; Zhang, Y.; Zhou, J.; Chen, Y.; Shang, R.; Luo, X. Adsorption capacity of kelp-like electrospun nanofibers immobilized with bayberry tannin for uranium(VI) extraction from seawater, *RSC Adv.* **2019**, *9*, 8091-8103.

(9) Yu, H.; Yang, S.; Ruan, H.; Shen, J.; Gao, C.; Van der Bruggen, B. Recovery of uranium ions from simulated seawater with palygorskite/amidoxime polyacrylonitrile composite, *Appl. Clay. Sci.* **2015**, *111*, 67-75.

(10) Zidan, W.I.; Abo-Aly, M.M.; Elhefnawy, O.A.; Bakier, E. Batch and column studies on uranium adsorption by amberlite XAD-4 modified with nano-manganese dioxide, *J. Radioanal. Nucl. Ch.* **2015**, *304*, 645-653.